

2 |

Feynman diagrams for spinless fields

In the previous chapter we have introduced relativistically invariant field theories. This chapter seeks to explain the role that these theories play in the description of interactions between elementary particles. In the course of this presentation we introduce Feynman diagrams, in terms of which one can describe a quantum field theory (at least in perturbation theory). We mainly concentrate on the ensuing particle interpretation and on the diagrammatical aspects. The construction of measurable quantities will be discussed in chapter 3.

2.1. External sources

It is a common strategy in physics to investigate the properties of a system by applying an external stimulus to it. One may, for example, study the properties of a crystal by examining the reaction of the displacement field to an external disturbance. Another example is from electrodynamics where one may study the effect of an electric current on electric and magnetic fields. In an analogous fashion we investigate the properties of a relativistic field theory, in this case the free massive Klein-Gordon theory, by examining the response of the field to a given external disturbance. Such a disturbance can be described by introducing an external source $J(x)$ to the Lagrangian (1.41),

$$\mathcal{L} = -\frac{1}{2}(\partial_\mu\phi)^2 - \frac{1}{2}m^2\phi^2 + J\phi, \quad (2.1)$$

where we note the analogy with the charge current and density in the electrodynamics Lagrangians (1.56) and (1.67). The source $J(x)$ will be some given function of x^μ . The equation of motion in the presence of the external source reads,

$$(\square - m^2)\phi(x) = -J(x). \quad (2.2)$$

To calculate the response to the disturbance caused by $J(x)$ we must solve this equation. Therefore we introduce the Green's function $\Delta(x - y)$, which is a solution of the equation

$$(\square - m^2)\Delta(x) = i\delta^4(x), \quad (2.3)$$

Using Dirac's representation of the δ -function

$$\delta^4(x) = (2\pi)^{-4} \int d^4k e^{ik \cdot x},$$

where $k \cdot x = \mathbf{k} \cdot \mathbf{x} - k^0 x^0$, and $d^4k = d^3k dk^0$, it is easy to construct the following solution for (2.3),

$$\Delta(x) = \frac{1}{i(2\pi)^4} \int d^4k \frac{e^{ik \cdot x}}{k^2 + m^2}. \quad (2.4)$$

Indeed,

$$\begin{aligned} (\square - m^2)\Delta(x) &= \frac{1}{i(2\pi)^4} \int d^4k (-k^2 - m^2) \frac{e^{ik \cdot x}}{k^2 + m^2} \\ &= i\delta^4(x). \end{aligned} \quad (2.5)$$

Note, however, that the integral (2.4) is not well-defined because the integrand has poles at $k^0 = \pm\omega(\mathbf{k})$, where $\omega(\mathbf{k}) = \sqrt{\mathbf{k}^2 + m^2}$. Ignoring this problem for the moment, we can use the Green's function to write the solution of (2.2) in the form

$$\phi(x) = \phi_0(x) + \int d^4y i\Delta(x-y)J(y), \quad (2.6)$$

where ϕ_0 is a solution of the source-free Klein-Gordon equation (i.e. (2.2) with $J = 0$).

To demonstrate how one obtains explicit solutions from (2.6) let us consider the case of a static point-like source located at \mathbf{r}_0 , i.e.,

$$J(\mathbf{x}, t) = g \delta^3(\mathbf{x} - \mathbf{r}_0). \quad (2.7)$$

Inserting (2.7) into (2.6) we find that the source causes a deviation from the source-free solution $\phi_0(x)$ equal to,

$$\begin{aligned} \delta\phi(x) &= ig \int d^4y \Delta(x-y) \delta^3(\mathbf{y} - \mathbf{r}_0) \\ &= \frac{g}{(2\pi)^3} \int d^3k \frac{e^{ik \cdot (\mathbf{x} - \mathbf{r}_0)}}{\mathbf{k}^2 + m^2}. \end{aligned}$$

Performing the integration over angular variables leads to

$$\delta\phi(x) = \frac{g}{2\pi^2} \frac{1}{r} \int_0^\infty dk \frac{k \sin kr}{k^2 + m^2}, \quad (2.8)$$

where $k = |\mathbf{k}|$ and $r = |\mathbf{x} - \mathbf{r}_0|$. Since the integrand is symmetric under $k \rightarrow -k$, we may also write,

$$\begin{aligned} \delta\phi(x) &= -\frac{ig}{4\pi^2 r} \int_{-\infty}^{+\infty} dk \frac{k e^{ikr}}{k^2 + m^2} \\ &= -\frac{ig}{8\pi^2 r} \int_{-\infty}^{+\infty} dk \left(\frac{1}{k + im} + \frac{1}{k - im} \right) e^{ikr}. \end{aligned} \quad (2.9)$$

This integral can be evaluated by contour integration in the upper half of the complex k plane. The final result reads

$$\delta\phi(x) = \frac{g}{4\pi r} e^{-mr} = \frac{g}{4\pi} \frac{e^{-m|\mathbf{x}-\mathbf{r}_0|}}{|\mathbf{x} - \mathbf{r}_0|}, \quad (2.10)$$

yielding a static disturbance to ϕ_0 with a characteristic range of order m^{-1} .

If we consider two sources, say localized at two different space-time points, then they will feel a mutual interaction due to the fact that the disturbance caused by one source will propagate to the second source and vice versa. This phenomenon can be compared to what happens when we attach mechanical devices at two different places to an elastic rod. The presence of these devices causes a disturbance to the vibrations that propagate through the rod, and both devices can feel the presence of one another through the propagation of these vibrations. Another example, which is more within the context of field theory, is the interaction of electric charges. Each charge causes an electric field which is felt by the other charge (as well as by the original charge itself). The Green's function $\Delta(x - y)$ describes the propagation of this field. For this reason it is often called the *propagator*.

Hence we have discovered that one important aspect of a field is to mediate a force between the sources that couple to it. As the field itself is only of secondary importance for this phenomenon, we may substitute the solution of the field equation back into the action and obtain an expression in terms of the sources only. To do this we write the action corresponding to (2.1) but now with two different sources J_1 , and J_2 as

$$S = \int d^4x \left\{ \frac{1}{2} \phi (\square - m^2) \phi + (J_1 + J_2) \phi - \frac{1}{2} \partial^\mu (\phi \partial_\mu \phi) \right\},$$

where the last term may be dropped because it depends only on the boundary of the integration domain by virtue of Gauss' theorem. Inserting now the result (2.6) of the field equation we find that the interaction between J_1 , and J_2 resides in the term

$$S^{\text{eff}}[J_1, J_2] = \int d^4x \int d^4y J_1(x) i\Delta(x - y) J_2(y), \quad (2.11)$$

Evaluating (2.11) for two static pointlike sources located at \mathbf{r}_1 and \mathbf{r}_2 (cf. 2.7) we find

$$S^{\text{eff}}[J_1, J_2] = \int dt \frac{g_1 g_2}{4\pi|\mathbf{r}_1 - \mathbf{r}_2|} e^{-m|\mathbf{r}_1 - \mathbf{r}_2|}, \quad (2.12)$$

where, for the moment, we assume that the time interval in (2.12) is finite. Hence (2.12) represents the interaction potential between two particles, say two nucleons coupling to the field ϕ . Precisely this potential was proposed by Yukawa in 1935, who conjectured the presence of a “meson” field as the mediator of the nuclear forces. From the range of that force he deduced the value of the mass parameter m to be about 100 MeV. In 1947 particles were found in this mass range, namely the pions. As it turned out, there exist both charged and neutral pions, with masses

$$\begin{aligned} m_{\pi^\pm} &= 139.5673 \pm 0.0007 \text{ MeV}/c^2, \\ m_{\pi^0} &= 134.9630 \pm 0.0038 \text{ MeV}/c^2. \end{aligned} \quad (2.13)$$

In the limit that $m = 0$ the integrand in (2.12) coincides with the electrostatic potential between two electric point charges g_1 and g_2 . As is well-known the Coulomb force has an infinite range, and is caused by the exchange of massless “photons”. Hence, we see that fields have also a particle interpretation. We thus discover two dual aspects: a field can act as the mediator of a force between two sources, and it can carry the degrees of freedom of a physical particle. In the next section we will further clarify this phenomenon.

2.2. Particles and propagators

Let us now consider the effect of an external source on the fields for time-dependent sources. In that case it is a meaningful question what will happen to the disturbance after the source has been switched off at a certain time (or has at least diminished substantially in strength). Hence we concentrate on the time behaviour of the corresponding field disturbance $\delta\phi$, written as (cf. 2.6),

$$\delta\phi(x) = \int d^4k \frac{e^{ik \cdot x}}{k^2 + m^2} J(k), \quad (2.14)$$

where $J(k)$ is the Fourier transform of $J(x)$ defined according to

$$J(x) = \int d^4k e^{ik \cdot x} J(k), \quad J(k) = (2\pi)^{-4} \int d^4x e^{-ik \cdot x} J(x). \quad (2.15)$$

Since $J(x)$ is real we have

$$J(k) = \bar{J}(-k), \quad (2.16)$$

where the bar indicates complex conjugation. To make the time dependence of (2.14) more explicit, we write

$$\delta\phi(x) = \int d^3k e^{i\mathbf{k}\cdot\mathbf{x}} \int dk^0 e^{-ik^0t} \frac{J(\mathbf{k}, k^0)}{\mathbf{k}^2 + m^2 - k^{02}}. \quad (2.17)$$

For large values of $|t|$ the factor e^{-ik^0t} in the integrand starts oscillating very rapidly so that one expects (2.17) to vanish. However, the example of the static source shows that this argument has to be applied with some care because in that case $\delta\phi$ turned out to be time-independent and non-vanishing. Here the Riemann-Lebesgue theorem is relevant, according to which

$$\lim_{t \rightarrow \infty} \int_{-\infty}^{\infty} dx f(x) e^{\pm itx} = 0,$$

when the integral $\int_{-\infty}^{+\infty} dx |f(x)|$ is finite. Therefore the integral (2.17) over k^0 should thus vanish for large $|t|$, provided the integrand $(\mathbf{k}^2 + m^2 - k^{02})^{-1} J(\mathbf{k}, k^0)$ is sufficiently regular. As already indicated above, this condition is obviously not satisfied for a static source where $J(\mathbf{k}, k^0)$ is proportional to $\delta(k^0)$. In the more general case the fact that the propagator exhibits poles at $k^0 = \pm\omega(\mathbf{k})$, where $\omega(\mathbf{k}) = \sqrt{\mathbf{k}^2 + m^2}$, is relevant. Due to them the disturbance (2.17) will not die out entirely, irrespective of whether the external source is square integrable. One will be left with contributions from the propagator poles, corresponding to plane waves whose energies and three-momenta satisfy the relativistic dispersion law $k^{02} - \mathbf{k}^2 - m^2 = 0$; those contributions are therefore expected to describe relativistic particles associated with the field ϕ . According to the above argument the contributions to the integral from momenta that do *not* satisfy $k^{02} - \mathbf{k}^2 - m^2 = 0$, are not able to manifest themselves at macroscopic time scales, i.e., at time scales larger than the intrinsic time scale over which the source varies. In contradistinction with *real* particles which are stable over an infinite time scale, those contributions are said to correspond to *virtual* particles. The aim of the subsequent discussion is to make some of this more precise.

Therefore let us investigate the behaviour of the integral

$$I(t) = \int_{-\infty}^{+\infty} dk^0 e^{-ik^0t} f(k^0), \quad (2.18)$$

for large time t , which can be determined by contour integration. For $t > 0$ we move the integration contour from the real axis to a distance a into the lower half of the complex k^0 -plane according to fig. 2.1. In general the function $f(k^0)$ will be such that the contributions from the vertical pieces of the contour C go to zero, so that we may write

$$I(t) = e^{-at} \int_{-\infty}^{+\infty} dk^0 e^{-ik^0t} f(k^0 - ia) + \oint_C dk^0 e^{-ik^0t} f(k_0). \quad (2.19)$$

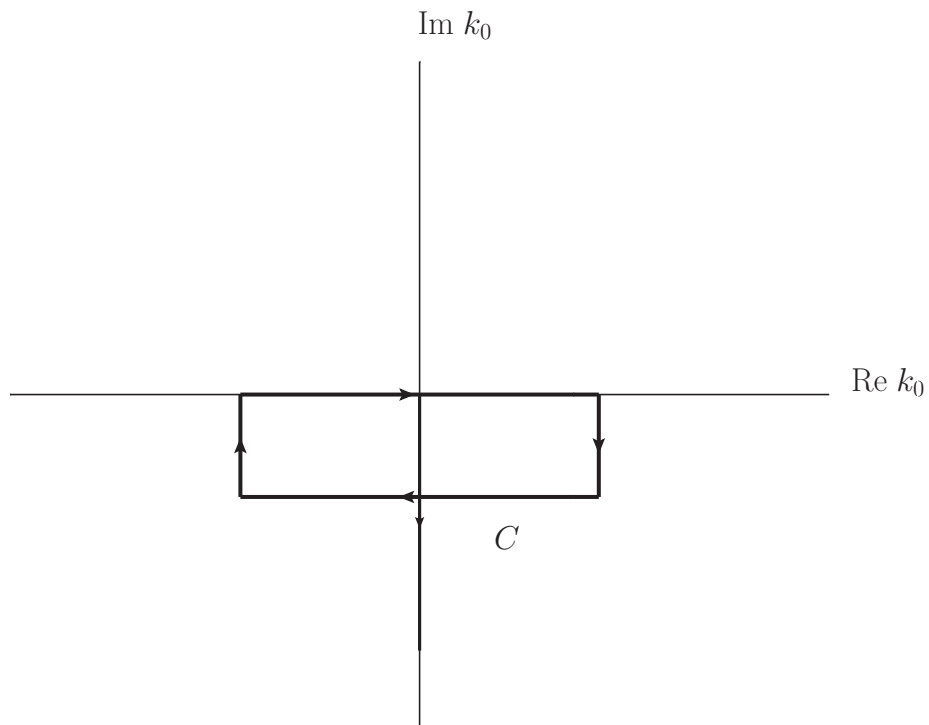


Figure 2.1: Integration contour in the complex k_0 -plane used in (2.19).

When the function has poles within the contour C , those will determine the dominant part of (2.18) at large positive times, because, according to Cauchy's residue theorem,

$$\oint_C dk^0 e^{-ik^0 t} f(k_0) = -2\pi i \sum_n e^{-i\omega_n t} \text{Res} f(\omega_n), \quad (2.20)$$

where the poles of $f(k^0)$ are located at $k^0 = \omega_n$. The pole closest to the real axis will thus determine the leading asymptotic behaviour of (2.18). The first term in (2.19) will be suppressed when a is taken large. Obviously we can apply the same argument for negative times. In that case we shift the integration contour into the upper k^0 -plane, and again the leading asymptotic behaviour is determined by the imaginary part of the pole that is closest to the real axis in the upper-half plane. Note that the contour has an opposite orientation in this case, so that the analogue of (2.20) carries an overall plus sign.

We now return to the k^0 -integral in (2.17), where the integrand exhibits poles on the real axis at $k^0 = \pm\omega(\mathbf{k})$. Since these poles are located on the real axis, we obviously need a prescription for how to integrate around these poles. As the mathematical structure of the theory does not provide any particular guidance, the choice must be based on physical arguments. From the previous discussion we can readily deduce the consequences. When we shift the poles at $k^0 = \pm\omega(\mathbf{k})$ by an infinitesimal amount into the *lower* half of the k^0 -plane, they will dominate the asymptotic behaviour of the integral at large *positive* time (we assume that the external source (2.17) is sufficiently regular so as not to affect this generic behaviour). The asymptotic time dependence is then governed by the pole residues $[\pm 2\omega(\mathbf{k})]^{-1} \exp[i(\mathbf{k} \cdot \mathbf{x} \mp \omega(\mathbf{k})t)]$ multiplied by $2\pi i J(\mathbf{k}, \pm\omega(\mathbf{k}))$. Alternatively, when we shift the poles by an infinitesimal amount into the upper k^0 -plane, they will dominate the asymptotic behaviour at large negative time with characteristic factors $[\mp 2\omega(\mathbf{k})]^{-1} \exp[i(\mathbf{k} \cdot \mathbf{x} \mp \omega(\mathbf{k})t)]$ again multiplied by $2\pi i J(\mathbf{k}, \pm\omega(\mathbf{k}))$.

We now attempt to interpret these contributions at $k^{02} - \mathbf{k}^2 - m^2 = 0$ as corresponding to quantum-mechanical waves that describe relativistic particles. Obviously, for positive time we would like to have only contributions of the form $[2\omega(\mathbf{k})]^{-1} \exp[i(\mathbf{k} \cdot \mathbf{x} - \omega(\mathbf{k})t)]$, corresponding to particles moving with momentum \mathbf{k} and energy $\omega(\mathbf{k})$. Consequently we shift the pole at $k^0 = \omega(\mathbf{k})$ to slightly *below* the real axis. It now seems reasonable to suppress the contribution of the pole at $k^0 = -\omega(\mathbf{k})$ at large positive time, so that we move this pole to slightly *above* the real axis (the integration contour in (2.17) is thus taken as indicated in fig. 2.2). How should one interpret the pole at $k_0 = -\omega(\mathbf{k})$ which now governs the behaviour for large negative time? Obviously the factor $[2\omega(\mathbf{k})]^{-1} \exp(i\mathbf{k} \cdot \mathbf{x} + i\omega(\mathbf{k})t)$ can be interpreted as a particle moving with momentum $-\mathbf{k}$ and energy $\omega(\mathbf{k})$. At first sight its exponential time dependence may seem to have the wrong sign, but it is

important to realize that this contribution to $\delta\phi(\mathbf{x}, t)$ now corresponds to a quantum-mechanical wave function which has been reconstructed from J by going *backwards* in time. We thus have the situation that the source $J(\mathbf{k})$ either emits an outgoing particle with momentum \mathbf{k} , or absorbs an incoming particle with momentum $-\mathbf{k}$. This interpretation, which was given by Stueckelberg and Feynman, indicates that the theory leads to a “causal” description, in spite of the fact that $\Delta(\mathbf{x}, t)$ does not vanish for $t < 0$.

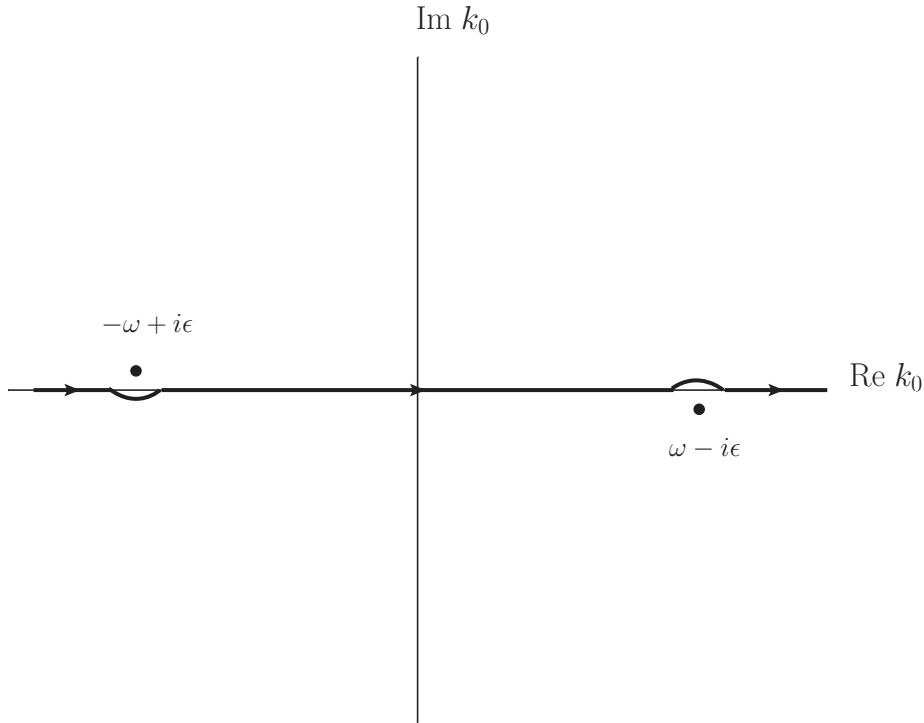


Figure 2.2: Displacement of the poles at $k_0 = \pm\omega(\mathbf{k})$ into the complex k_0 -plane.

In order to describe the complete process of emission and absorption we recall (2.11),

$$S^{\text{eff}}[J_1, J_2] = \int d^4x_1 d^4x_2 J_1(x_1) i\Delta(x_1 - x_2) J_2(x_2).$$

This expression can be pictorially presented by means of a diagram as shown in fig. 2.3, where the line between the two sources denotes the propagator $\Delta(x_1 - x_2)$. Such diagrams are called Feynman diagrams. We now assume

Figure 2.3: Feynman diagram representing $S^{\text{eff}}[J_1, J_2]$.

that both sources are localized in time and separated by a timelike distance, such that $t_1 - t_2 > 0$. If this time difference is larger than the intrinsic time scale set by the time variations of the sources, then (2.11) can be approximated by

$$S^{\text{eff}}[J_1, J_2] \stackrel{t_1 - t_2 \rightarrow \infty}{\approx} i(2\pi)^{-3} \int \frac{d^3 k}{2\omega(\mathbf{k})} \int d^3 x_1 d^3 x_2 dt_1 dt_2 \\ \times J_1(\mathbf{x}_1, t_1) \exp[i\mathbf{k} \cdot (\mathbf{x}_1 - \mathbf{x}_2) - i\omega(\mathbf{k})(t_1 - t_2)] J_2(\mathbf{x}_2, t_2). \quad (2.21)$$

This is just the contribution from the propagator pole in the lower-half complex k^0 -plane (see fig. 2.2). Equation (2.21) describes a particle with momentum $P^\mu = k^\mu = (\mathbf{k}, \omega(\mathbf{k}))$ emitted by J_2 and subsequently absorbed by J_1 . The amplitude for this process is thus proportional to $J_1(-P)J_2(P)$, or, since the sources are real, to $\bar{J}_1(P)J_2(P)$.

Now consider the same expression (2.11) with $t_1 - t_2$ large and negative. In this case, the propagator pole in the upper complex k_0 -plane (see fig. 2.2) contributes and we find

$$S^{\text{eff}}[J_1, J_2] \stackrel{t_2 - t_1 \rightarrow \infty}{\approx} i(2\pi)^{-3} \int \frac{d^3 k}{2\omega(\mathbf{k})} \int d^3 x_1 d^3 x_2 dt_1 dt_2 \\ \times J_1(\mathbf{x}_1, t_1) \exp[i\mathbf{k} \cdot (\mathbf{x}_1 - \mathbf{x}_2) + i\omega(\mathbf{k})(t_1 - t_2)] J_2(\mathbf{x}_2, t_2). \quad (2.22)$$

This describes precisely the alternative situation, namely a particle with momentum $P_\mu = -k_\mu = (-\mathbf{k}, \omega(\mathbf{k}))$ exchanged between J_1 and J_2 , but now emitted by J_1 and subsequently absorbed by J_2 . The corresponding amplitude is proportional to $\bar{J}_1(-P)J_2(-P)$. As one may expect on physical grounds the overall sign of (2.21) and (2.22) is the same, which is a consequence of the fact that the two propagator poles have been shifted to opposite halves of the complex k^0 -plane.

Hence expression (2.11) and the corresponding Feynman diagram in fig. 2.3 describe two possible processes for sources separated by a large difference in time. These two possibilities, namely absorption or emission of a particle by one source, and the prior emission or subsequent absorption of this particle by the other source, are summarized in fig. 2.4. The left graph shows the momentum assignment after Fourier transforming (2.11). For large positive $t_1 - t_2$, a particle is emitted by the source $J_2(P)$ and absorbed by $J_1(P)$,

where $k = P$. This contribution is represented by (2.21) and follows from the positive-energy propagator pole, i.e. $k^0 > 0$. For large negative $t_1 - t_2$, a particle is emitted by $J_1^*(-P)$ and absorbed by $J_2(-P)$, where $k = -P$. This contribution, given in (2.22), corresponds to the negative-energy propagator pole, i.e. $k^0 < 0$.

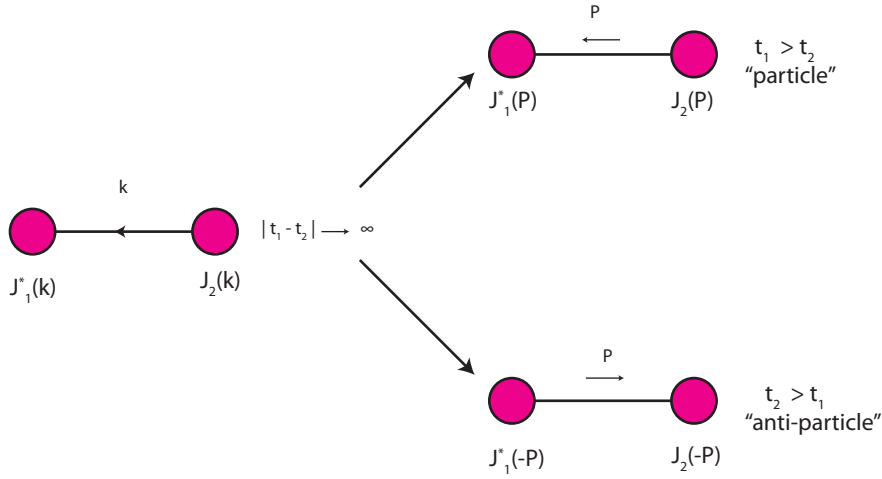


Figure 2.4: Emission and absorption of particles and antiparticles by external sources.

It is standard terminology to associate the contribution from the negative-energy propagator pole with a so-called *antiparticle*. In the case at hand the distinction between particle and antiparticle is superficial, as the field and its corresponding source are real [i.e. $J(-P) = J^*(P)$]. This is not so for complex fields. Complex fields are necessary when one deals with particles that carry electric charge. The reason is that charged fields transform under electromagnetic gauge transformations, which take the form of phase transformations. Such transformations can only be realized on complex fields. One of the consequences is that ϕ and ϕ^* correspond to particles of opposite electric charge. The analysis of the interaction of two sources (cf. 2.21- 2.22) remains the same, except that also the sources are now complex. Introducing a coupling

$J\phi^* + J^*\phi$ into the Lagrangian $\mathcal{L} = -|\partial_\mu\phi|^2 - m^2|\phi|^2$, one finds

$$S^{\text{eff}}[J_1^*, J_2] = \int d^4x_1 d^4x_2 J_1^*(x_1) i\Delta(x_1 - x_2) J_2(x_2). \quad (2.23)$$

If the sources are localized and have a large timelike separation, (2.23) describes the emission of a charged particle by J_2 and its subsequent absorption by \bar{J}_1 if $t_1 - t_2 > 0$, or the emission of an antiparticle (which has opposite charge) by J_1^* and its absorption by J_2 if $t_1 - t_2 < 0$. Note that fig. 2.4 still remains applicable, but now particles and antiparticles are no longer the same since there is no relation anymore between J and J^* . It is important to realize that the propagator now carries an *orientation*, referring to the flow of charge, i.e., positive charge from 1 to 2 or negative charge from 2 to 1. The orientation of the propagator is usually indicated by an arrow on the lines in the corresponding Feynman diagram. This charge flow arrow should be distinguished from the arrow that defines the momentum flow through the propagator line (although so far in our definition the two coincide). If a particle is exchanged from J_2 to \bar{J}_1 the momentum of the propagator line coincides with the particle momentum, i.e. $P^\mu = k^\mu$, with $k^0 = \omega(\mathbf{k})$. For an antiparticle going from \bar{J}_1 to J_2 one has $P^\mu = -k^\mu$, with $k^0 = -\omega(\mathbf{k})$, precisely as exhibited in fig. 2.4.

Hence we understand the two dual aspects of a field. On the one hand a field mediates a force by the exchange of “virtual” particles. On the other hand, certain modes of the field (i.e. those associated with the propagator poles) describe real physical particles. Both these aspects are contained in the causal propagator, which we have defined by means of the integration contour of fig. 2.2. Precisely this choice of the contour is implemented by writing the propagator as

$$\Delta(x - y) = \frac{1}{i(2\pi)^4} \int d^4k \frac{e^{ik \cdot (x-y)}}{k^2 + m^2 - i\varepsilon}, \quad (2.24)$$

where the limit $\varepsilon \downarrow 0$ is to be performed at the end of the calculation. Note that this limiting procedure is manifestly Lorentz invariant.

For future purposes we now evaluate the positive and negative frequency parts of (2.24) by contour integration in the complex k^0 -plane. For $x^0 > 0$ we can close the integration contour by a half circle in the lower-half plane, for $x^0 < 0$ we can close it in the upper half plane (see fig. 2.5). The contributions along the half circles vanish, and we find

$$\begin{aligned} \Delta(x) &= \frac{i}{(2\pi)^4} \int d^3k e^{i\mathbf{k}\cdot\mathbf{x}} \int_{C_-} dk_0 \frac{e^{-ik_0 x^0}}{k_0^2 - \omega(\mathbf{k})^2 + i\varepsilon}, \quad x^0 > 0, \\ \Delta(x) &= \frac{i}{(2\pi)^4} \int d^3k e^{i\mathbf{k}\cdot\mathbf{x}} \int_{C_+} dk_0 \frac{e^{-ik_0 x^0}}{k_0^2 - \omega(\mathbf{k})^2 + i\varepsilon}, \quad x^0 < 0, \end{aligned} \quad (2.25)$$

Using Cauchy's residue theorem we find that the pole at $k^0 = \omega(\mathbf{k}) - i\varepsilon$ determines the integral for $t > 0$, and the pole at $k^0 = -\omega(\mathbf{k}) + i\varepsilon$ the integral for $t < 0$ (note that we consistently drop terms of order ε^2). The result can be written as

$$\Delta(x) = \theta(x^0)\Delta^+(x) + \theta(-x^0)\Delta^-(x), \quad (2.26)$$

where $\theta(t)$ is a step function defined by

$$\theta(x^0) = \begin{cases} 1 & \text{for } x^0 > 0, \\ 0 & \text{for } x^0 < 0, \end{cases} \quad (2.27)$$

and Δ^\pm are given by

$$\begin{aligned} \Delta^+(x) &= \frac{1}{(2\pi)^3} \int \frac{d^3k}{2\omega(\mathbf{k})} e^{i\mathbf{k}\cdot\mathbf{x} - i\omega(\mathbf{k})x^0}, \\ \Delta^-(x) &= \frac{1}{(2\pi)^3} \int \frac{d^3k}{2\omega(\mathbf{k})} e^{i\mathbf{k}\cdot\mathbf{x} + i\omega(\mathbf{k})x^0}. \end{aligned} \quad (2.28)$$

Δ^+ (Δ^-) can be interpreted as the contribution from particles (antiparticles) going from 0 to x (x to 0). For later use note the following identities),

$$\begin{aligned} \Delta^\pm(x) &= (2\pi)^{-3} \int d^4k \delta(k^2 + m^2) \theta(\pm k^0) e^{ik\cdot x}, \\ \Delta^+(-x) &= [\Delta^+(x)]^* = \Delta^-(x). \end{aligned} \quad (2.29)$$

2.3. Pion scattering by an electromagnetic potential

To demonstrate the use of Feynman diagrams in a more complicated situation, we discuss the scattering of charged pions by an electromagnetic potential. The latter should be thought of as a given field $A_\mu(x)$ which is weak and vanishes outside a localized region of space-time. This field could for instance be generated by the charge distribution of an atom. Since the pions are charged they are described by a complex field ϕ . The Lagrangian describing the interaction with the vector potential A_μ , is generated by the usual "minimal substitution" $\partial_\mu\phi \rightarrow (\partial_\mu - iqA_\mu)\phi$ in (1.78), which yields

$$\begin{aligned} \mathcal{L} &= -\partial_\mu\phi^* \partial^\mu\phi - m^2\phi^*\phi - iqA_\mu(\phi^* \partial^\mu\phi - \phi \partial^\mu\phi^*) - q^2 A_\mu^2 \phi^*\phi \\ &\quad + J^*\phi + J\phi^*. \end{aligned} \quad (2.30)$$

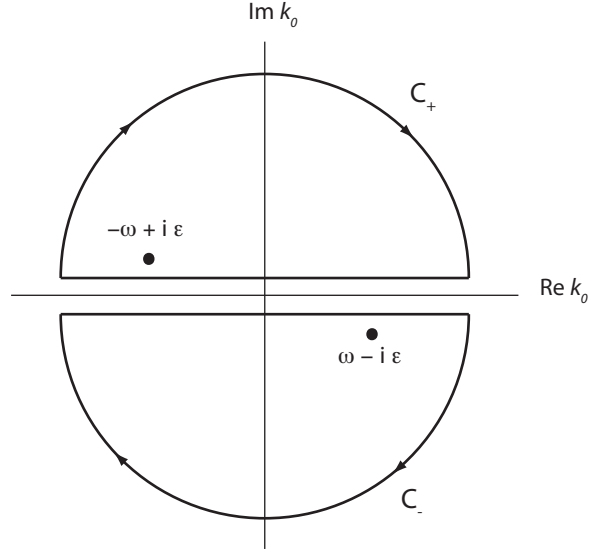


Figure 2.5: The contours C_+ and C_- in the complex k^0 -plane used in (2.25).

The charge of π^+ is denoted by q . The equations of motion corresponding to this Lagrangian follow from Hamilton's principle (see chapter 1; here A_μ is a given function which need not be varied). The result reads

$$(\square - m^2)\phi = - [J - 2iq A_\mu \partial^\mu \phi - iq \phi \partial^\mu A_\mu - q^2 A_\mu^2 \phi] . \quad (2.31)$$

This equation can again be written as an integral equation by making use of the Green's function $\Delta(x)$. Indeed,

$$\begin{aligned} \phi(x) = & \phi_0(x) + \int d^4y i\Delta(x-y) \\ & \times [J(y) - 2iq A_\mu(y) \partial^\mu \phi(y) - iq \phi(y) \partial^\mu A_\mu(y) - q^2 A_\mu^2(y) \phi(y)] , \end{aligned} \quad (2.32)$$

where ϕ_0 is a solution of the free Klein-Gordon equation.

It is possible to solve (2.32) by iteration in a way that is analogous to the usual derivation of the Born series in non-relativistic quantum mechanics. To that order one substitutes the lowest-order solution,

$$\phi^{(0)}(x) = \phi_0(x) + \int d^4y i\Delta(x-y)J(y) ,$$

back into the right-hand side of (2.32). This leads to a first-order approximation,

$$\begin{aligned} \phi^{(1)}(x) &= \phi_0(x) + \int d^4y i\Delta(x-y)J(y) \\ &\quad + \int d^4y i\Delta(x-y) [-2iq A_\mu(y) \partial^\mu - iq \partial^\mu A_\mu(y) - q^2 A_\mu^2(y)] \\ &\quad \times \left[\phi_0(y) + \int d^4z i\Delta(y-z)J(z) \right]. \end{aligned} \quad (2.33)$$

The n -th order approximation is then found by substituting the $(n-1)$ -th order approximation into (2.32):

$$\begin{aligned} \phi^{(n)}(x) &= \phi_0(x) + \int d^4y i\Delta(x-y)J(y) \\ &\quad + \int d^4y i\Delta(x-y) [-2iq A_\mu(y) \partial^\mu - iq \partial^\mu A_\mu(y) - q^2 A_\mu^2(y)] \phi^{(n-1)}(y). \end{aligned} \quad (2.34)$$

Let us now assume that the vector potential is weak so that it is justified to retain only the first-order contribution in (2.34) and discard the A_μ^2 term. We concentrate on the following term in (2.33)

$$\begin{aligned} \delta\phi(x) &= - \int d^4y i\Delta(x-y) \\ &\quad \times \left[2iq A_\mu(y) \frac{\partial}{\partial y^\mu} + iq \partial^\mu A_\mu(y) \right] \int d^4z i\Delta(y-z)J(z), \end{aligned} \quad (2.35)$$

which represents a response of the field to the external source in the presence of the electromagnetic potential. If we repeat the same steps that led to (2.11), and reinsert (2.35) back into the Lagrangian, we find that the interaction between the two external sources J_1 and J_2 is changed in the presence of the electromagnetic field. In lowest order this effect is given by

$$\begin{aligned} S^{\text{eff}}[J_1^*, J_2] &= \int d^4x J_1^*(x) \int d^4y i\Delta(x-y) \\ &\quad \times \left[-2iq A_\mu(y) \frac{\partial}{\partial y_\mu} - iq \partial^\mu A_\mu(y) \right] \int d^4z i\Delta(y-z) J_2(z). \end{aligned} \quad (2.36)$$

Again (2.36) may be expressed pictorially by a Feynman diagram, as is shown in fig. 2.6. Precisely as before, such a diagram may describe a variety of different physical situations. If the sources and the electromagnetic potential are not separated by sufficiently large timelike distances then (2.36) describes the

effect of the potential on the interaction between the two external sources; hence (2.36) represents the first-order correction to the result previously described in section 2.1. This situation can be described in terms of virtual particles mediating the force between the sources, which are now affected by the presence of the electromagnetic potential.

In the case that the sources and the vector potential have a large timelike separation, the Feynman diagram describes a variety of physical processes involving π^+ - and π^- -particles. We assume here that the interaction induced by the vector potential is localized in time; this is a standard assumption to ensure that the asymptotic states can be treated as free particles. In fact, in a rigorous treatment of time-independent interactions one always makes use of a limiting procedure, by which the interaction is switched off adiabatically at large times. However, these subtleties are ignored in this discussion. The

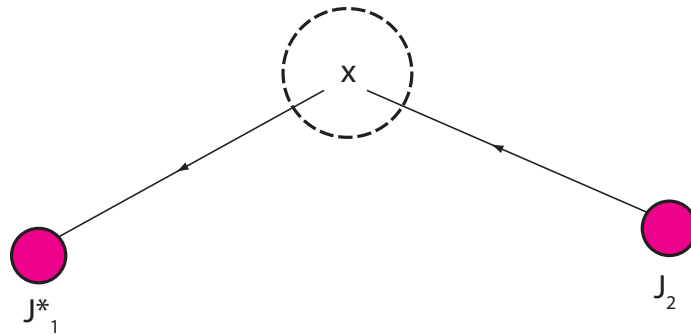


Figure 2.6: Feynman diagram describing scattering and annihilation reactions of pions interacting with an electromagnetic potential.

diagram of fig. 2.6 and its corresponding expression (2.36) do not yet specify a particular sequence of events; for every temporal sequence we may distinguish a corresponding physical process:

(a) *Scattering of positively charged pions:*

If the timelike separations between the interactions with A_μ , and the sources J_1^* and J_2 is such that $t_2 \ll t_i$ and $t_1 \gg t_i$, where t_1 and t_2 denote the characteristic times at which the sources are operative and t_i denotes the characteristic time at which the interaction with the potential occurs, then fig. 2.6 describes the scattering of π^+ by an external potential: the particle is emitted by J_2 , scatters off the potential, and is subsequently absorbed by J_1 .

(b) *Scattering of negatively charged pions:*

If the sequence of events is precisely the opposite then fig. 2.6 describes the scattering of the anti-particle π^- : the anti-particle is emitted by J_1^* , scatters off the potential, and is absorbed by J_2 .

(c) *Annihilation:*

We now consider the case where the characteristic times of J_1^* and J_2 are prior to the time of the interaction. In that case a particle is emitted by J_2 , and an antiparticle by J_1^* . In the interaction with the external source both π^+ and π^- are absorbed.

(d) *Pair creation:*

In this case both J_1^* and J_2 are separated from the interaction with the potential in such a way that both $t_1, t_2 > t_i$. Now we have a particle absorbed by J_1 and an anti-particle by J_2 , which has been created by the interaction prior to the absorption.

The four processes mentioned above are not all experimentally realizable. There is no problem with scattering; pion beams can be created in the laboratory and charged pions can be scattered off, say the electromagnetic field of a heavy nucleus, just as in classical Rutherford scattering. The electromagnetic potential for a static field is $A_\mu(x) = (\mathbf{0}, A_0(\mathbf{x}))$, where for Coulomb scattering one has $A_0(\mathbf{x}) \propto |\mathbf{x} - \mathbf{r}|^{-1}$. In such a situation the pion is deflected in the Coulomb field with no change in the magnitude of its three-momentum.

For pair creation the potential must be such that enough energy is released to create a particle-antiparticle pair, i.e. $E > 2m_\pi$. This is not a static situation but one can imagine an excited nuclear level (the difference in energy between atomic levels is too small) which is unstable and generates a potential. Usually of course, lighter mass electron-positron pairs would be produced more copiously. Any surplus energy above the threshold $E = 2m_\pi$ goes into the kinetic energy of the recoiling particles. The annihilation channel is physically more difficult to measure but a Gedanken experiment is possible. For instance one can imagine a situation where an incoming π^+ and π^- annihilate each other near an atom (or nucleus), with all the released energy going into the creation of a highly excited atom (nucleus). The potential needed to do this is clearly nonstatic because there is an absorption of energy.

All four processes are described by the same expression (2.36). The relevant formula is obtained by taking the Fourier transform of (2.36) and subsequently ignoring the external source attachments and the corresponding propagators. The reason we drop the sources and the propagators is that we are interested in what happens between emission and absorption and not in how the particles are precisely emitted and absorbed. This is just what corresponds to an experimental situation, where one tries to extract the result of the measurement in a way that is independent of the characteristic features of the particle beams, the target and the detectors. The precise relation between the resulting amplitude and quantities that are more closely related to the actual measurement, such as cross sections and decay rates, is discussed in chapter 3.

Defining the Fourier transform of $A_\mu(x)$ by

$$A_\mu(x) = \int d^4p e^{ip \cdot x} A_\mu(p),$$

it is straightforward to show that (2.36) takes the form

$$\begin{aligned} S^{\text{eff}}[J_1^*, J_2] &= -i \int d^4k_1 d^4k_2 [i(2\pi)^4 J_1^*(k_1)] [i(2\pi)^4 J_2(k_2)] \\ &\quad \times \left(\frac{1}{i(2\pi)^4 k_1^2 + m^2 - i\varepsilon} \right) V(k_1, k_2) \left(\frac{1}{i(2\pi)^4 k_2^2 + m^2 - i\varepsilon} \right), \end{aligned} \quad (2.37)$$

where $V(k_1, k_2)$ describes the interaction vertex

$$V(k_1, k_2) = i(2\pi)^4 \int d^4p \delta(k_2 + p - k_1) (-iq) (2ik_2 + ip)^\mu A_\mu(p). \quad (2.38)$$

In (2.37) we have not yet cancelled the factors of $[i(2\pi)^4]^{-1}$ coming from the definition of the propagators (cf. 2.24). Every source attachment involves a momentum-conserving delta function and is accompanied by a factor of $(2\pi)^4$. Since every iteration involves a factor of i , we consistently associate a factor of $i(2\pi)^4$ with every vertex together with a momentum conserving delta function. This leaves an overall factor of $-i$ in (2.37).

The momentum factor $i(2k_2 + p)^\mu$, is the result of the derivative $\partial/\partial y^\mu$, acting on the propagator attached to J_2 and on A_μ . The momenta k_1 and k_2 are assigned to the propagator lines, such that the charge flow and the momentum flow coincide. According to the previous considerations, (2.38) describes four different situations, depending on how we choose the relation between propagator momenta and particle momenta. The four possible momentum assignments are as follows:

(a) *Scattering of positively charged pions:*

Here k_2 is the incoming π^+ -momentum, and k_1 the outgoing π^+ -momentum, with $(k_1)^0 = \omega(\mathbf{k}_1)$, $(k_2)^0 = \omega(\mathbf{k}_2)$.

(b) *Scattering of negatively charged pions:*

Here $-k_1$ is the incoming π^- -momentum, and $-k_2$ the outgoing π^- -momentum, with $(k_1)^0 = -\omega(\mathbf{k}_1)$, $(k_2)^0 = -\omega(\mathbf{k}_2)$.

(c) *Annihilation:*

Here $-k_1$ is the incoming π^- -momentum, and k_2 the incoming π^+ -momentum, with $(k_1)^0 = -\omega(\mathbf{k}_1)$, $(k_2)^0 = \omega(\mathbf{k}_2)$.

(d) *Pair creation:*

Here k_1 is the outgoing π^+ -momentum, and $-k_2$ the outgoing π^- -momentum, with $(k_1)^0 = \omega(\mathbf{k}_1)$, $(k_2)^0 = -\omega(\mathbf{k}_2)$.

The fact that four different processes can be defined from one formula is usually called *crossing*. This property is manifest when one makes use of Feynman diagrams.

2.4. Feynman rules for spinless fields

We will now introduce the graphical representation in terms of Feynman diagrams in a more systematic fashion. As a starting point consider a model described by the Lagrangian,

$$\mathcal{L} = -\frac{1}{2}(\partial_\mu\phi)^2 - \frac{1}{2}m^2\phi^2 - g\phi^3 + J\phi, \quad (2.39)$$

where we have included a self-interaction for the fields, as well as an external source. The field equations corresponding to (2.39) read

$$(\square - m^2)\phi = -(J - 3g\phi^2), \quad (2.40)$$

which, by again using the propagator function $\Delta(x)$, can be written as an integral equation

$$\phi(x) = \phi_0(x) + \int d^4y i\Delta(x-y)[J(y) - 3g\phi^2(y)]. \quad (2.41)$$

Ignoring $\phi_0(x)$, which is a solution of the free Klein-Gordon equation $(\square - m^2)\phi_0 = 0$, we solve (2.41) by iteration, just as we have described in the previous section. This yields an expansion, of which we give the first few terms,

$$\begin{aligned} \phi(x) = & \int d^4x_1 i\Delta(x-x_1)J(x_1) \\ & + \int d^4x i\Delta(x-x_1)(-3g) \int d^4x_2 i\Delta(x_1-x_2) \\ & \times \left[J(x_2) - 3g \int d^4x_4 i\Delta(x_2-x_4)J(x_4) \int d^4x_5 i\Delta(x_2-x_5)J(x_5) \right] \\ & \times \int d^4x_3 i\Delta(x_1-x_3) \\ & \times \left[J(x_3) - 3g \int d^4x_6 i\Delta(x_3-x_6)J(x_6) \int d^4x_7 i\Delta(x_3-x_7)J(x_7) \right] \\ & + \dots \end{aligned} \quad (2.42)$$

The various terms in (2.42) can be represented graphically as follows. Every propagator $\Delta(x-y)$ corresponds to a line connecting the space-time points x and y ; every self-interaction or interaction with an external source or a potential at a given space-time point corresponds to a vertex. In this way the expansion (2.42) can be represented as in fig. 2.7. In these graphs an integration over all space time points except x is implied.

The meaning of these diagrams is intuitively clear. The source J causes fluctuations of the field at various places which propagate to the space-time

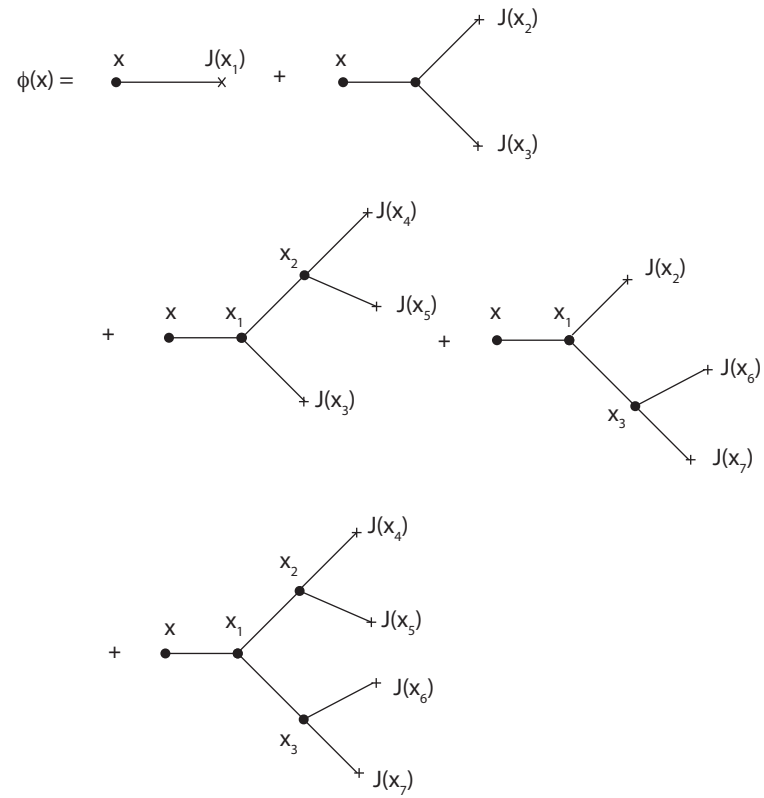


Figure 2.7: Diagrammatic representation of (2.42).

point x where ϕ is measured. During this propagation there are the mutual interactions described by the vertices of the diagrams. In a more picturesque way one may say that the source emits virtual particles which propagate to x after a number of interactions with other virtual particles emitted by the same source at different space-time points. In the course of these interactions (virtual) particles can be created or annihilated. However, this picture may lead to incorrect conclusions when taken too literally, because the space-time intuition that one has for physical particles does not always apply to virtual particles.

At this stage it is obvious why Feynman diagrams play such an important role. The analytic expression corresponding to each diagram is complicated and difficult to disentangle because of the many integration parameters. The diagram, on the other hand, concisely encodes the formula, and more importantly allows one to grasp its meaning immediately. The diagrams of fig. 2.7 are called “tree” diagrams for obvious reasons. We will encounter only tree diagrams as long as we attempt to solve the equations of motion in perturbation theory. For a consistent quantum field theory, however, one must also include diagrams with closed loops, such as shown in fig. 2.8. One can prove that each closed loop in a Feynman diagram gives rise to a factor \hbar , although this is not obvious in our considerations since we have taken $\hbar = 1$ from the start. Taking into account diagrams with closed loops thus corresponds to including the quantum-mechanical corrections to the theory in question. We will not give a systematic derivation for diagrams with closed loops. To do this requires a thorough discussion of the *quantization* of the theory. This quantization can be done in various different ways. One method is based on path integrals and uses functional methods. Another approach, called canonical quantization, is based on the Hamiltonian and regards fields as operators in an abstract Hilbert space. A discussion of these methods is outside the scope of this book and we refer the interested reader to more advanced text books and review papers.

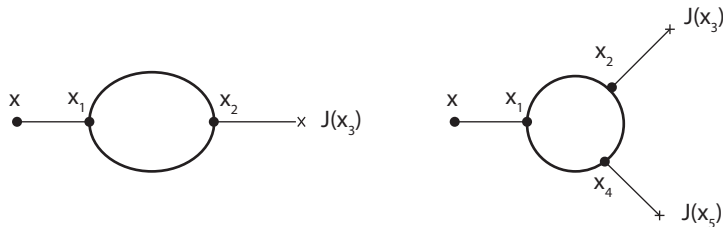


Figure 2.8: Examples of diagrams with closed loops.

In section 2.6 we will further elaborate on the physical implications of dia-

grams with closed loops. Here we just note that the analytic expression corresponding to the loop diagrams of fig. 2.8 is

$$\begin{aligned} \phi(x) = & 18g^2 i^4 \int d^4x_1 d^4x_2 d^4x_3 \\ & \times \Delta(x-x_1) \Delta(x_2-x_1) \Delta(x_1-x_2) \Delta(x_2-x_3) J(x_3) \\ & - 216g^3 i^6 \int d^4x_1 d^4x_2 d^4x_3 d^4x_4 d^4x_5 \\ & \times \Delta(x-x_1) \Delta(x_1-x_2) \Delta(x_2-x_3) \\ & \times \Delta(x_2-x_4) \Delta(x_4-x_1) \Delta(x_4-x_5) J(x_3) J(x_5), \end{aligned} \quad (2.43)$$

where the combinatorial factors will be discussed shortly in a slightly different context. Again, observe how concisely a Feynman diagram describes the structure of a cumbersome mathematical expression.

Because we will always deal with field theories that are translationally invariant, it is convenient to discuss the theory in the momentum representation in which the momenta of physical particles are defined. In order to find the precise prescription for writing down the mathematical expressions corresponding to a given diagram, let us examine the various factors that arise when one writes one of the terms in (2.42) in the momentum representation. Using the Fourier transform in four dimensions,

$$\begin{aligned} \phi(x) &= \int d^4k e^{ik \cdot x} \phi(k), \\ \phi(k) &= (2\pi)^{-4} \int d^4x e^{-ik \cdot x} \phi(x). \end{aligned} \quad (2.44)$$

we write the second diagram in fig. 2.7 as

$$\begin{aligned} & -3g \int d^4x_1 i\Delta(x-x_1) \int d^4x_2 i\Delta(x_1-x_2) J(x_2) \int d^4x_3 i\Delta(x_1-x_3) J(x_3) \\ &= -3g \int d^4k \frac{1}{k^2 + m^2 - i\varepsilon} e^{ik \cdot x} \int d^4k_1 \int d^4k_2 \delta^4(k - k_1 - k_2) \\ & \quad \times \frac{1}{k_1^2 + m^2 - i\varepsilon} J(k_1) \frac{1}{k_2^2 + m^2 - i\varepsilon} J(k_2). \end{aligned} \quad (2.45)$$

Every propagator now has an assigned momentum variable, and a four-dimensional delta-function appears at each vertex, so that energy-momentum is conserved. Because there are three propagators, two sources and one vertex, the factors of $i(2\pi)^4$ cancel in this expression.

Now we plan to generalize the rules for diagrams. The aim is to define diagrams and their corresponding mathematical expressions for a general field theory. To do this one may keep the source attachments of the external lines,

so that the diagrams can be viewed as contributions to the effective interaction between a number of these sources; a typical diagram is given in fig. 2.9. Since these diagrams are generalizations of the propagator diagrams which have two external lines they are called generalized *Green's functions*. An n -point Green's function is the sum of all possible diagrams, including both tree diagrams and diagrams with closed loops, with n external lines. A common restriction is to sum only over *connected* diagrams, i.e. diagrams which cannot be divided into two parts without cutting at least one internal line. Ultimately we shall be interested in the *invariant amplitude* which follows from the connected Green's function by removing the sources and the propagators that connect the sources to the main part of the diagram. The invariant amplitude corresponds directly to the quantum mechanical probability amplitude that describes a certain physical process as we will discuss in the next chapter. We will then also derive the corresponding expressions for physically measurable quantities such as cross sections and decay rates.

Figure 2.9: Graphical representation of the five-point Green's function.

We should emphasize that Feynman diagrams have a wider range of applicability than just elementary particle physics, and are equally useful in many-body theory and statistical mechanics. However, Feynman diagrams are mainly used in the context of perturbation theory. Thus they may not represent the full quantum field theory which often has solutions that are not amenable to weak-coupling expansions.

We now present the Feynman rules for writing down diagrams in a general theory.

- (1) Begin with a field theory defined in terms of an action, which is expressed as an integral over space-time of the Lagrangian.
- (2) Calculate the propagators of the theory, which follow from the terms in the

action that are quadratic in the fields. The quadratic terms define a matrix in momentum space which is diagonal in the momentum variables [owing to the translational invariance of the theory (see problem 2.1)]. Suppose we take the Lagrangian (2.39) as an example. The action is

$$\begin{aligned} S &= \int d^4x \mathcal{L} \\ &= \int d^4x \left[-\frac{1}{2}(\partial_\mu \phi)^2 - \frac{1}{2}m^2 \phi^2 + O(\phi^3) \right]. \end{aligned} \quad (2.46)$$

Now take the Fourier transform of the part which is quadratic in the fields. We find that this yields the term

$$S = -\frac{1}{2}(2\pi)^4 \int d^4k \phi^*(k) (k^2 + m^2) \phi(k), \quad (2.47)$$

where we have made use of the fact that we are dealing with real fields [i.e. $\phi^*(k) = \phi(-k)$]. Hence the elements of the diagonal matrix are just equal to $-\frac{1}{2}(2\pi)^4(k^2 + m^2)$. For real fields the propagator is defined as a factor $\frac{1}{2}i$ times the inverse of this matrix. For the case at hand we thus find

$$\Delta(k) = \frac{1}{i(2\pi)^4} \frac{1}{k^2 + m^2 - i\epsilon}, \quad (2.48)$$

which is diagrammatically written as a line, with an arrow indicating the momentum flow. The $i\epsilon$ -term has been discussed before.

For complex fields the standard normalization is different. In that case the kinetic terms in the action are

$$\begin{aligned} S &= \int d^4x \mathcal{L} \\ &= \int d^4x \left(-|\partial_\mu \phi|^2 - m^2|\phi|^2 \right), \end{aligned} \quad (2.49)$$

and taking the Fourier transform leads to [we no longer have $\phi^*(k) = \phi(-k)$]

$$S = -(2\pi)^4 \int d^4k \phi^*(k) (k^2 + m^2) \phi(k). \quad (2.50)$$

The propagator is now defined by the inverse of $-(2\pi)^4(k^2 + m^2)$ multiplied by a factor i . This leads to the same diagram as for real fields, but now the arrow also indicates that the propagator is oriented in the sense that the endpoints of the propagator lines refer to independent fields; the standard convention is that incoming arrows refer to ϕ , and outgoing ones to ϕ^* . Of course, complex fields can be regarded as a linear combination of two real fields, and by decomposing $\phi = \frac{1}{2}\sqrt{2}(\phi_1 + i\phi_2)$ one makes contact with the description given

for real fields (see problem 2.4).

(3) The next step is to define the vertices of the graphs. We associate a vertex with n lines with every term in the Lagrangian that contains n powers of the field. In the beginning of this section we have already seen that a Lagrangian with a ϕ^3 term yields a vertex with three lines. Translational invariance ensures that the Fourier transform yields a delta-function in momentum space, thus guaranteeing energy-momentum conservation as was, for instance, explicitly shown in (2.45). Each vertex thus corresponds to

$$\text{vertex} = i(2\pi)^4 \delta^4 \left(\sum_j k_j \right) \times (\text{coefficient of } \phi^n \text{ in the Lagrangian}), \quad (2.51)$$

where our conventions are such that the k_j denote the *incoming* momenta associated with each of the fields. For example, the Feynman rules for the theory described by the Lagrangian

$$\mathcal{L} = -\frac{1}{2}(\partial_\mu \phi)^2 - \frac{1}{2}m^2 \phi^2 - \lambda \phi^3 - g \phi^4, \quad (2.52)$$

are summarized in table 2.1.

$$\text{vertices: } i(2\pi)^4 \delta^4(k_1 + i-, +k_3)(-i)$$

Table 2.1: Feynman rules corresponding to the Lagrangian

1

When the vertices in the Lagrangian contain derivatives then each differentiation of the fields contributes a factor ik_j to the vertex where k_j is the *incoming* momentum of the j -th line. These momentum factors are part of the coefficient indicated in the generic definition (2.51). Thus the terms $g \phi^3$ and $g \phi (\partial_\mu \phi)^2$ both correspond to three-point vertices, but yield different factors: $i(2\pi)^4 g \delta^4(k_1 + k_2 + k_3)$ and $i(2\pi)^4 g (-k_2 \cdot k_3) \delta^4(k_1 + k_2 + k_3)$, respectively. In the latter case the choice of the second and the third momentum as those corresponding to the differentiated fields, is arbitrary. A complete calculation must also include other possible line attachments, so that also factors $(-k_1 \cdot k_3)$ and $(-k_1 \cdot k_2)$ will contribute. The way in which these contributions must be summed will be discussed next, but it is rather obvious in this case that the total contribution of the second interaction becomes proportional to $(k_1 \cdot k_2 + k_2 \cdot k_3 + k_3 \cdot k_1)$.

¹Observe that we do not include combinatorial factors to account for the fact that external lines can be connected to a vertex in different ways.

In the Feynman diagrams for complex fields the lines at the vertices carry an orientation; recall that fields correspond to lines with incoming arrows and their complex conjugates to lines with outgoing arrows. A formulation in terms of complex rather than real fields is useful if the theory is invariant under phase transformations, i.e.

$$\phi \rightarrow \phi' = e^{i\alpha} \phi.$$

In that case every interaction must contain an equal number of fields ϕ and their complex conjugates ϕ^* , so that each vertex must contain an equal number of incoming and outgoing lines. The lines coming from the vertices can now only be joined if their orientational arrows match (as discussed in section 2.3 the orientation often corresponds to the flow of electric charge; obviously, charge will be conserved if the number of incoming and outgoing arrows is the same at each vertex).

(4) One now joins all the lines emanating from the vertices via propagators in order to form the various diagrams. The external lines may be attached to external sources. The momentum flow through the various lines is determined by the momentum-conserving δ -functions at the vertices, and for real fields one may readjust the arrows in order to reflect this fact. An example of this is shown in fig. 2.10. If we write the propagator as $-i(2\pi)^{-4}D(p)$ and the vertices as $i(2\pi)^4\delta^4(p_1 + p_2 + p_3)\Gamma(p_1, p_2, p_3)$ with incoming momenta p_1, p_2, p_3 , then the diagram formed in fig. 2.10 leads to Diagram(fig. 2.10)

$$\begin{aligned} &\propto i(2\pi)^4\delta(p_1 + p_2 + p_3 + p_4 + p_5)D(-p_2 - p_3)D(-p_4 - p_5) \\ &\times \Gamma(p_1, p_2 + p_3, p_4 + p_5)\Gamma(p_2, p_3, p_1 + p_4 + p_5)\Gamma(p_4, p_5, p_1 + p_2 + p_3). \end{aligned}$$

If the arrow denotes more than just the momentum assignment of the lines, but also the orientation (e.g. charge flow) then the lines cannot always be joined, and the number of possible diagrams will be reduced.

The rules given so far apply to diagrams with closed loops as well. However, in this case not all the momenta of the internal lines are fixed by momentum conservation, and one is left with one or more unrestricted momenta over which one should integrate. Figure 2.11 shows an example of such a situation, which, in the same notation as above, leads to Diagram(fig. 2.11)

$$\propto \int d^4k \Gamma(p, k, -p - k)\Gamma(-p, -k, p + k)D(k)D(-p - k),$$

where we have no longer written an overall δ -function for the external momenta. Note that unlike the previous case there is no left-over factor of $i(2\pi)^4$ because there are equal numbers of propagators and vertices (propagators for

Figure 2.10: Construction of a tree diagram from propagators and vertices.

external lines have not been included). We will discuss the meaning of diagrams with closed loops at the end of this chapter.

(5) Finally one sums over all possible diagrams with the same configuration of external lines. In order to do so one must determine the combinatorial weight factor associated with each of the diagrams. In principle this weight factor counts the number of ways in which a diagram can be formed by connecting vertices to propagators and external lines, but diagrams that only differ in the position of the vertices are counted as identical (because we ultimately integrate over all vertex positions in space-time).

Figure 2.11: Construction of a loop diagram from propagators and vertices.

Diagrams obtained by interchanging external lines attached to different vertices do not always lead to identical expressions. To see this consider again the diagram of fig. 2.10 as an example. The three vertices are distinguished by the fact that they are each connected to different external lines (namely to the lines with momentum p_1 , or p_2 and p_3 , or p_4 and p_5). Given the structure of the diagram there are 6 different ways to connect the three (internal and external) lines to the vertex, so that the weight factor is equal to $6^3 = 216$. Diagrams such as fig. 2.12a should be added as independent diagrams. They

carry their own weight factor (which is also equal to 216) and correspond to a different analytic expression because the momenta flowing through the internal lines are different from those in fig. 2.10. Diagram 2.12b on the other hand is just identical to the diagram of fig. 2.10, by an interchange of vertices, and should *not* be counted separately.

Figure 2.12: The connection of propagators and vertices to form diagrams (a) inequivalent and (b) equivalent to the diagram in fig. 2.10.

There is only one exception to the above counting argument. If identical vertices occur in an indistinguishable way, i.e. not distinguished by their attachments to external lines, then one must avoid overcounting by dividing by $n!$, where n is the number of such indistinguishable vertices. Rather than discussing these rules in as general a way as possible, we prefer to consider a specific and more realistic calculation in the next section. To allow the reader to test his/her ability in determining these combinatorial factors, we have presented a few specific examples for the theory described by (2.52) in table 2.2. We recall that if one deals with fields that carry an orientation, some of the ways of forming the diagrams will now be forbidden, which will reflect itself in the combinatorial weights.

-6 λ

Table 2.2: Examples of combinatorial factors for various diagrams following from the Lagrangian (2.52).

Before turning to a model calculation let us add some further comments. The fact that we integrate over the momentum variable associated with closed loops is consistent with the above criteria. Since we sum over all possible diagrams, we must also sum over all possible momentum configurations (i.e. all

momenta that are left unrestricted by momentum conservation). Likewise we must also sum over all types of internal lines that are possible. As we will learn later, particles with spin are described by multicomponent fields (for example, for spin-1 particles one uses a vector field, similar to the electromagnetic vector potential that we have introduced in the previous chapter). The propagator for such a field is then a matrix, and the corresponding propagator line has an index assigned to both endpoints. If such a propagator appears in a Feynman diagram then one must sum over all field components. In principle the Feynman rules introduced above encompass all these cases. There is one exception: for closed loops formed by a string of fermion propagators one must introduce a factor -1, and there are similar complications for fermionic external lines. These complications do not reflect themselves in the diagrammatic representation and follow from independent considerations. We return to this point in chapter 5.

Note that although we have initially constructed the (tree) diagrams by considering an iterative solution to the field equation, we have deviated from this starting point when we defined the Feynman rules. The above prescription leads to the n -point Green's functions of the theory. We are ultimately interested in the invariant amplitude which follows from the connected Green's functions by truncation of the external lines.

2.5. An example: pion-pion scattering

Although pion-pion scattering is not easy to study in the laboratory because we have no stable targets made of pions, this process can be studied indirectly by considering certain related reactions. Theoretically the subject is of some interest because a lot of information on reactions that involve pions can be derived from so-called soft-pion theorems, which are based on the observation that the relatively low mass of the pion can be understood from an approximate chiral symmetry. We will examine such a soft-pion result later in this section.

For our purpose pion-pion scattering is a suitable process to demonstrate the application of the Feynman rules because we avoid the complications of particles with spin. We will calculate the pion-pion scattering amplitude on the basis of a model. Before introducing this model we note that three kinds of pions exist in Nature. There is the neutral pion (π^0) and the two charged pions (π^\pm) with masses given in (2.13). The charged pions can be represented by a complex field, as was done previously in section 2.3. However, it is sometimes convenient to express this field in terms of two real fields, i.e.

$$\pi^\pm \rightarrow \frac{\phi^1 \mp i\phi^2}{\sqrt{2}}. \quad (2.53)$$

The field of the neutral pion is real, and is then denoted by ϕ^3 . In view of the fact that the pions have nearly equal masses, it is natural to combine the fields into a three-dimensional vector field

$$\phi = (\phi_1, \phi_2, \phi_3), \quad (2.54)$$

and to contemplate the application of transformations that rotate the vector ϕ . These rotations are called *isospin* transformations.

Isospin, an abbreviation of the term “isobaric spin” was introduced by Heisenberg in the context of the proton-neutron system. Because the proton and the neutron have almost equal masses, he suggested to combine them into a doublet structure. The proton-neutron doublet then transforms under isospin transformations in the same way as a doublet of spin- $\frac{1}{2}$ states transform under rotations. The mass degeneracy of the proton and the neutron is then understood from the approximate invariance under isospin transformations. Historically it was then realized that the nuclear forces do not distinguish between protons and neutrons; hence they must be invariant under isospin transformations. Since the nuclear forces arise mainly as the result of virtual pion exchange the pions must be subject to the same isospin transformations, and this fact leads to the assignment of the pions to an isovector representation as is expressed by (2.54). Of course the electromagnetic interactions are not invariant under isospin transformations because they couple differently to charged and neutral pions. This suggests that the electromagnetic interactions are in fact responsible for the slight difference in mass between π^0 and π^\pm , or proton and neutron. According to more modern views this is, however, only partially the case and there are other independent reasons for these mass differences.

The model that we will use for the calculation of this section is based on the pion fields ϕ , and a single field denoted by σ . The pions behave as pseudoscalars under parity reversal, and we assume that the hypothetical sigma particle is a scalar meson, viz.

$$\begin{aligned} \phi(\mathbf{x}, t) &\xrightarrow{P} \phi^P(\mathbf{x}, t) = -\phi(-\mathbf{x}, t), \\ \sigma(\mathbf{x}, t) &\xrightarrow{P} \sigma^P(\mathbf{x}, t) = \sigma(-\mathbf{x}, t). \end{aligned} \quad (2.55)$$

The most general Lagrangian that preserves isospin and parity reversal with coupling constants of nonnegative dimension, is given by

$$\begin{aligned} \mathcal{L} = & -\frac{1}{2}(\partial_\mu \phi)^2 - \frac{1}{2}m^2 \phi^2 - \frac{1}{2}(\partial_\mu \sigma)^2 - \frac{1}{2}\mu^2 \sigma^2 \\ & - \lambda \sigma \phi^2 - g(\phi^2)^2 - g' \sigma^2 \phi^2 - \lambda' \sigma^3 - g'' \sigma^4. \end{aligned} \quad (2.56)$$

In (2.56) we have five interaction terms with coupling constants g, g', g'', λ and λ' . The masses of the pion and sigma mesons are m and μ , respectively.

The Feynman rules corresponding to (2.56) are summarized in table 2.3. The propagators and vertices follow from the prescription given in the previous

section, but we have not yet accounted for the fact that one can connect the lines to the vertices in a variety of ways (often one writes the vertices such that the various combinations and their corresponding weight factors are included explicitly; we refrain from doing this as it is precisely this aspect that we want to exhibit here).

Table 2.3: Feynman rules corresponding to the Lagrangian (2.56)^a

2

Figure 2.13: The four-pion vertex.

In tree approximation only two types of diagrams contribute to the amplitude for pion-pion scattering. There is a direct interaction that follows from the $g^2(\phi^2)^2$ vertex, and an exchange reaction with a virtual sigma between two $\sigma \phi^2$ vertices. Let us first concentrate on the first diagram. We assume four external pion lines with isospin indices a, b, c and d , and corresponding momenta p^a, p^b, p^c and p^d (see fig. 2.13). Since we intend to describe pion-pion scattering we choose p^a and p^b incoming and p^c and p^d outgoing. The total contribution corresponding to fig. 2.13 is now determined as follows. First there is the standard $i(2\pi)^4\delta^4(p^a + p^b - p^c - p^d)$ times the coupling constant $(-g)$. We then have to see in how many different ways the external lines can be attached to the vertex. Clearly there are 4 ways to connect the first line with isospin label a . For the second line, say with label b , there are two possibilities. One may begin by connecting the second line to the field which was contracted with the field associated with the first line. In that case we find a factor δ^{ab} , and the third and fourth line also correspond to a contracted pair of fields. There are then two ways left to contract these lines with labels c and d , which gives an extra factor 2, so that this combination finally yields

²Observe that we do not include combinatorial factors to account for the fact that external lines can be connected to the vertices in different ways. In the expression for the pion-pion vertex the inequivalent line attachments are indicated by dots.

$4 \cdot 2 \delta^{ab} \delta^{cd}$. The second possibility is to contract the second line with label b to a field that was not contracted with the field associated with the first line. There are two different ways to do this, and the labels a and b now remain independent. To connect the third and fourth line there are again two options left: either c should coincide with a , and d with b , or c should coincide with b , and d with a . Therefore we arrive at $4 \cdot 2 (\delta^{ac} \delta^{bd} + \delta^{ad} \delta^{bc})$. Adding all terms the total contribution corresponding to the diagram of fig. 2.13 is therefore

$$\begin{aligned} \text{Diagram}(\text{fig. 2.13}) &= -i(2\pi)^4 \delta^4(p^a + p^b - p^c - p^d) \\ &\quad \times 8g(\delta^{ab} \delta^{cd} + \delta^{ac} \delta^{bd} + \delta^{ad} \delta^{bc}). \end{aligned} \quad (2.57)$$

To verify the correctness of this result one may of course select certain values for the indices a, b, c and d , and explicitly consider the possible diagrams writing the interaction $-g(\phi^2)^2$ explicitly as $-g(\phi_1^2 + \phi_2^2 + \phi_3^2)^2$. Note that altogether (2.57) contains 24 combinations (each combination of Kronecker delta's appears with a factor 8), which is exactly the number of ways in which one can attach four lines to a four-point vertex. The 24 combinations are sometimes explicitly included in writing down the Feynman rules as in table 2.3. This is mainly a matter of convenience, and since we will usually consider relatively simple diagrams, we prefer to work out the various combinations for each graph separately.

Figure 2.14: Tree diagrams with σ -exchange contributing to pion-pion scattering.

The next step is to consider the σ -exchange diagrams, which are shown in fig. 2.14. There are clearly three such diagrams because the pion line with label a can be connected with either one of the three other pion lines through a $\sigma\phi^2$ vertex. Again we have the usual factor $i(2\pi)^4$ times the δ -function at each of the vertices. But in this case we must also include the propagator for the σ -field. Therefore we are left with only one factor $i(2\pi)^4$, an overall δ -function, $\delta^4(p^a + p^b - p^c - p^d)$, and a propagator factor $(k_\sigma^2 + \mu^2)^{-1}$, where k_σ is the momentum associated with the internal σ line. This momentum is different for each of the diagrams in fig. 2.14. For the first diagram we have $k_\sigma = p^a + p^b$, for the second $k_\sigma = p^a - p^c$, and for the third $k_\sigma = p^a - p^d$. What remains is to determine the combinatorial factors, which is straightforward in this case. At each of the vertices the two pion lines can be hooked onto the

vertex in two different ways. Hence we find $4\delta^{ab}\delta^{cd}$, $4\delta^{ac}\delta^{bd}$, $4\delta^{ad}\delta^{bc}$ for the three diagrams respectively, and the result for the diagrams of fig. 2.14 takes the form

$$\begin{aligned} \text{Diagrams (fig. 2.14)} &= i(2\pi)^4 \delta(p^a + p^b - p^c - p^d) \\ &\times 4\lambda^2 \left\{ \frac{\delta^{ab}\delta^{cd}}{(p^a + p^b)^2 + \mu^2} + \frac{\delta^{ac}\delta^{bd}}{(p^a - p^c)^2 + \mu^2} + \frac{\delta^{ad}\delta^{bc}}{(p^a - p^d)^2 + \mu^2} \right\}. \end{aligned} \quad (2.58)$$

The sum of (2.57) and (2.58) now leads to the total amplitude in tree approximation.

At this point it is convenient to introduce so-called Mandelstam variables.

$$s = -(p^a + p^b)^2, \quad t = -(p^a - p^c)^2, \quad u = -(p^a - p^d)^2. \quad (2.59)$$

It is easy to show that

$$s + t + u = -(p^a)^2 - (p^b)^2 - (p^c)^2 - (p^d)^2,$$

so that for physical pions

$$s + t + u = 4m^2, \quad (2.60)$$

The invariant amplitude for pion-pion scattering is obtained by removing the factor $i(2\pi)^4 \delta(p^a + p^b - p^c - p^d)$ in (2.57) and (2.58), and can be written as

$$\mathcal{M}(\pi^a + \pi^b \rightarrow \pi^c + \pi^d) = \delta^{ab}\delta^{cd}F(s) + \delta^{ac}\delta^{bd}F(t) + \delta^{ad}\delta^{bc}F(u), \quad (2.61)$$

where the function $F(x)$ equals

$$F(x) \equiv 4 \left\{ \frac{\lambda^2}{\mu^2 - x} - 2g \right\}. \quad (2.62)$$

Let us now briefly contemplate the case of zero pion mass. One can then rigorously take the “soft-pion limit”, where the four-momentum of one of the pions is taken to zero. In that limit $s, t, u \rightarrow 0$, so that the amplitude (2.61) takes the form

$$\mathcal{M}(\pi^a + \pi^b \rightarrow \pi^c + \pi^d) = F(0)(\delta^{ab}\delta^{cd} + \delta^{ac}\delta^{bd} + \delta^{ad}\delta^{bc}).$$

This shows that if $2g = \lambda^2/\mu^2$ then the whole amplitude vanishes and pions do not scatter from each other. To see the significance of this choice of parameters we note that the relation between the coupling constants λ and g is precisely reproduced by the following Lagrangian

$$\begin{aligned} \mathcal{L} &= -\frac{1}{2}((\partial_\mu \phi)^2 + (\partial_\mu \sigma)^2) + \frac{1}{2}(\phi^2 + (\sigma + v)^2) \\ &\quad - g(\phi^2 + (\sigma + v)^2)^2 + (\sigma^3, \sigma^4 \text{ and } \sigma^2 \phi^2 \text{ terms}), \end{aligned} \quad (2.63)$$

where

$$v = \sqrt{\frac{\mu^2}{8g}}.$$

The form of (2.63) clearly suggests a more symmetric Lagrangian, for which the unspecified σ^3, σ^4 and $\sigma^2\phi^2$ terms are ignored. The field can then be combined into a four-component vector

$$\phi_{(4)} = (\phi, \sigma + v),$$

and under arbitrary rotations of this vector the Lagrangian is left invariant. This particular model is known as the sigma model (see problem 2.6). In this model the isospin transformations, which form a three-dimensional rotation group, are thus extended to the four-dimensional rotation group, SO(4). We note that the mass term of the Lagrangian (2.63) has the “wrong” sign, apparently leading to the relativistic dispersion relation $E^2 = \mathbf{p}^2 - m^2$ implying that the particles travel at velocities larger than that of light. However, we have already understood that this is deceptive; collecting all ϕ^2 and σ^2 terms in (2.63) leads to zero-mass pions and sigma mesons with mass μ . The “wrong” sign only arises when we insist on writing the Lagrangian in its SO(4) symmetric form. We shall see later that the wrong sign for the mass term is a signal for spontaneous breakdown of a symmetry, which leads to massless particles according to Goldstone’s theorem. The SO(4) invariant realization is not stable in this case.

2.6. Quantum corrections

Although it is often sufficient to restrict oneself to a calculation of all relevant tree diagrams it is important that we understand the nature of diagrams with closed loops. For the sake of the argument we will pretend for the moment that all loop diagrams are well-defined (this is not really so, as we shall see in chapter 8 where the difficulties caused by divergent loop diagrams will be discussed). We have already mentioned that loop diagrams represent the quantum-mechanical corrections to a classical field theory. Even although the initial Lagrangian is relatively simple, the full quantum theory, where we sum over all possible diagrams, is extremely complicated. This is so because the momentum integrals that occur for diagrams with closed loops give rise to expressions that contain nontrivial functions of the external momenta. The effective interaction between particles is therefore no longer given in terms of simple vertex functions but in terms of nontrivial functions of the momenta, the coupling constants and the mass parameters from the initial Lagrangian. This implies that the parameters of this Lagrangian no longer have a direct

physical meaning. To be specific let us, for instance, consider the σ - π - π vertex in the model of the previous section. In tree approximation this vertex is just given by the coupling constant λ , but to this initial vertex one must now add all possible diagrams with one external sigma and two external pion lines. This is shown in fig. 2.15. Hence the effective σ - π - π vertex corresponding to the sum of all these diagrams takes the form

$$\Gamma(p_\sigma, p^a, p^b) = i(2\pi)^4 \delta^4(p_\sigma + p^a + p^b) \delta^{ab} \{ \lambda + \dots \}, \quad (2.64)$$

where the dots represent the closed-loop graphs; in principle, these graphs can be calculated order by order in perturbation theory.

Figure 2.15: Diagrams representing the quantum corrections to the σ - π - π vertex.

It is possible to understand these results in terms of an intuitive picture. The Feynman diagrams, such as in fig. 2.15, show how particles continuously emit and absorb “virtual particles”, thereby becoming virtual particles themselves. Hence the nature of a physical particle changes; rather than being a single pointlike object, it behaves more like a composite system of virtual particles. According to the arguments given in section 2.2 these virtual constituents cannot exist for more than a short instant of time, so they cannot be observed directly. Their effect, however, can be seen indirectly, for instance by probing this cloud of virtual particles with another particle or some external field. In that case the effective interaction that one measures will indicate that one is dealing with a composite object with a finite extension in space. To see this we recall that if a pointlike object is hit by another particle, the only effect is that its momentum will be changed in a way that is consistent with energy–momentum conservation, and the strength of the interaction is insensitive to the momentum that is transferred in the collision process. Taking into account only the lowest-order vertex in (2.64), which is constant, corresponds to this case. On the other hand, for a composite object the strength of the interaction will depend on the momentum transfer; when the object is probed at higher momenta the nature of the interaction will change as a result of the inner structure. This explains the nontrivial dependence on the momenta that is generated by the loop diagrams. This momentum dependence is usually characterized in terms of certain functions called *form factors*.

It is sometimes possible to give a more physical interpretation of these form factors. To see this let us return to the scattering of charged pions by an electromagnetic potential. Suppose that the pion is deflected in the Coulomb field of a heavy nucleus. The scattering process is described by the diagram of fig. 2.16, and the Coulomb potential arises as the result of the photon propagator at finite spacelike momentum this follows from setting $m = 0$ in (2.12)]. To reproduce the exact Coulomb potential one must assume that the photon nucleus vertex does not depend on the virtual photon momentum, since this would effectively modify the photon propagator. This assumption amounts to treating the nucleus as an elementary pointlike object. The form factor that one would measure in this case would thus be constant. Obviously this may be a good approximation at small momentum transfer where the nucleus is hit only very gently, but if the nucleus is probed harder then its nature as a composite system will become apparent. Since the virtual photon probes the electric charge distributed in the nucleus, this distribution reflects itself in the behaviour of the nucleus form factor which in fact is precisely the Fourier transform of the charge distribution. Indeed, for a pointlike particle, the charge is concentrated at a single point so that the charge distribution is a delta function whose Fourier transform is simply a constant. Consequently the form factor for a pointlike particle is momentum independent.

Figure 2.16: Diagram representing electromagnetic scattering of a pion on a nucleus.

In the example of a nucleus we understand a great deal of what is responsible for the form factor, since the nucleus may be thought of as a bound state of protons and neutrons. In a field-theoretic context the form factors arise from the contributions of Feynman diagrams with closed loops, and can be viewed as the result of the presence of a cloud of virtual particles that is present at any instant of time.

It should be emphasized that there is no essential contradiction between bound states of physical particles and these composite states formed from virtual particles. Strictly speaking the word particle always refers to an object that is stable, i.e. that can exist for an infinite amount of time not subjected

to any kind of external forces. Once such a particle is trapped inside, say, a nucleus, it loses some of its characteristic features. Its mass, for instance, which is defined by the relativistic dispersion law $E(\mathbf{p}) = \sqrt{\mathbf{p}^2 + m^2}$ in the absence of external forces, has no longer an intrinsic meaning. Inside the nucleus the particle becomes “virtual”, i.e. it is no longer confined to its free particle mass shell.

How then does one determine the mass of a physical particle. If it must be viewed as a cloud of virtual particles which are constantly being created or annihilated? To understand this we recall the relation between propagators and physical particles that we have discussed in section 2.2. Physical particles were shown to be associated with the poles in the propagator, because only fluctuations with momenta corresponding to these poles could manifest themselves over asymptotically large time scales. However, we must now consider the full propagator which includes all possible Feynman diagrams with two external lines. We have indicated some of those diagrams in fig. 2.17 for the pion propagator in the model of the previous section. At first sight it

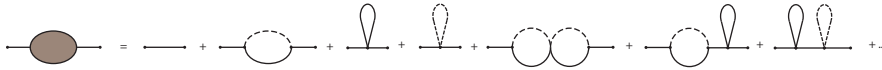


Figure 2.17: Diagrams contributing to the full pion propagator.

seems that the full propagator will now also exhibit multiple poles, because there are diagrams consisting of a chain of subdiagrams connected by single propagator lines which carry the momentum of the external lines. A typical example of such a diagram is fig. 2.18a. However, the appearance of these multiple poles is deceptive. To see this we first divide all possible diagrams into (“one-particle”) irreducible and reducible ones. A diagram is called irreducible if it cannot be divided into two disconnected diagrams by cutting only one internal line. This internal line must carry the momentum assigned to the full propagator; the attachment of a so-called “tadpole” diagram shown in fig. 2.18c leads to an internal line with zero momentum, which is therefore not counted as a reducible diagram. Obviously, diagram 2.18b is also irreducible, whereas diagram 2.18a is not.

We now consider the sum of all irreducible diagrams contributing to the propagators, which we denote by $\Sigma(p)$. In $\Sigma(p)$ we have neither included the propagators associated with the two external lines nor the lowest-order

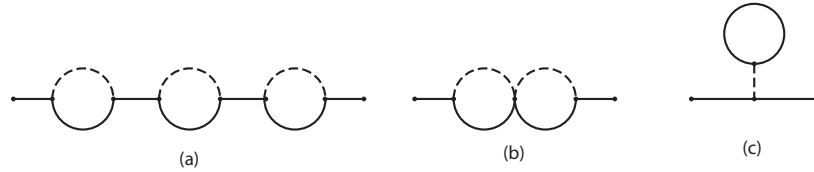


Figure 2.18: Example of self-energy diagrams. Diagram (a) is reducible, while diagrams (b) and (c) are irreducible.

propagator itself. The full propagator can now be expressed in terms of $\Sigma(p)$ by summing the graphs as indicated in fig. 2.19. The corresponding expression reads

$$\begin{aligned} \Delta(p) &= \frac{1}{i(2\pi)^4} \frac{1}{p^2 + m^2} + \frac{1}{i(2\pi)^4} \frac{1}{p^2 + m^2} \Sigma(p) \frac{1}{i(2\pi)^4} \frac{1}{p^2 + m^2} \\ &+ \frac{1}{i(2\pi)^4} \frac{1}{p^2 + m^2} \Sigma(p) \frac{1}{i(2\pi)^4} \frac{1}{p^2 + m^2} \Sigma(p) \frac{1}{i(2\pi)^4} \frac{1}{p^2 + m^2} + \dots \end{aligned} \quad (2.65)$$

This result constitutes a geometric series which can easily be summed. The

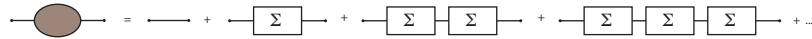


Figure 2.19: The full propagator $\Delta(p)$ expressed in terms of the irreducible self-energy diagrams $\Sigma(p)$.

full propagator then takes the form

$$\Delta(p) = \frac{1}{i(2\pi)^4} \frac{1}{p^2 + m^2 - \frac{1}{i(2\pi)^4} \Sigma(p)}. \quad (2.66)$$

Hence we understand that the multiple poles in (2.65) are just the result of truncating an infinite series of terms generated by (2.66).

The mass of the physical particles in the full quantum theory is now associated with the poles in the propagator (2.66). Hence the mass is no longer given by the mass parameter m in the Lagrangian, but instead it is a solution M of the equation

$$M^2 = m^2 - \frac{1}{i(2\pi)^4} \Sigma(p)|_{p^2 = -M^2}. \quad (2.67)$$

In general this equation is hard to solve, but in perturbation theory it can be solved by iteration.

Hence we see that the continuous emission and absorption of the virtual quanta changes the mass of the physical particle. This change is determined by the diagrams contained in $\Sigma(p)$. For that reason $\Sigma(p)$ is called the *self-energy*, i.e. the extra amount of rest-mass energy that is generated by the interactions. The summation procedure leading to (2.66), which is called the Dyson equation, allows one to consistently take these effects into account. We should also mention that the function $\Sigma(p)$ is in general not analytic in the momentum p , and the poles are also not necessarily at real values of M^2 . If the latter is the case then the relation between particles and propagators that we have discussed in section 2.2 will be changed, and it will turn out that we are dealing with unstable particles. This will be discussed in the next chapter when we define the decay rate for unstable particles.

Problems

2.1. Under a constant translation, $\phi(\mathbf{x}) \rightarrow \phi'(\mathbf{x}) = \phi(\mathbf{x} - \boldsymbol{\xi})$, the corresponding transformation for the Fourier transform reads $\phi(\mathbf{k}) \rightarrow \phi'(\mathbf{k}) = \exp(i\mathbf{k} \cdot \boldsymbol{\xi}) \phi(\mathbf{k})$. Argue now that for a translation-invariant theory propagators should only depend on a single momentum vector, as was asserted in the text preceding (2.46). Show also that momentum must be conserved at every vertex.

2.2. Consider a real scalar field ϕ with the Lagrangian

$$\mathcal{L} = -\frac{1}{2}(\partial_\mu \phi)^2 - \frac{1}{2}m^2 \phi^2 - \lambda \phi^3 - g \phi^4.$$

Draw the one-loop and two-loop diagrams which contribute to the self-energy for ϕ . Show that the combinatorial factors for the diagrams given below are both equal to $2^6 3^3$.

2.3. Consider the Lagrangian $\mathcal{L} = \mathcal{L}_0 + \mathcal{L}_1$ for a scalar field ϕ . Here \mathcal{L}_0 is the Lagrangian for a free field with mass m ,

$$\mathcal{L}_0 = -\frac{1}{2}(\partial_\mu \phi)^2 - \frac{1}{2}m^2 \phi^2,$$

and \mathcal{L}_1 describes the interactions,

$$\mathcal{L}_1 = -g \phi [2(\partial_\mu \phi)^2 + m^2 \phi^2] - g^2 \phi^2 [2(\partial_\mu \phi)^2 + \frac{1}{2}m^2 \phi^2].$$

Write down the Feynman rules for this theory. Calculate the lowest-order amplitudes with three and four external lines and show that they vanish on the mass shell, i.e., when the external momenta satisfy $p^2 = -m^2$. Explain this result by performing a field redefinition of the type

$$\phi \rightarrow \phi' = a \phi + b \phi^2 + c \phi^3 + \dots$$

2.4. The Lagrangian

$$\mathcal{L} = -\frac{1}{2}(\partial_\mu\phi_1)^2 - \frac{1}{2}(\partial_\mu\phi_2)^2 - \frac{1}{2}m^2(\phi_1^2 + \phi_2^2). \quad (1)$$

can be written as

$$\mathcal{L} = -|\partial_\mu\phi|^2 - m^2|\phi|^2, \quad (2)$$

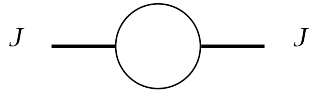
with $\sqrt{2}\phi = \phi_1 + i\phi_2$. The propagators corresponding to (1) are,

$$\Delta_{ab}(p) = \frac{1}{i(2\pi)^4} \frac{\delta_{ab}}{p^2 + m^2 - i\epsilon}, \quad a, b = 1, 2. \quad (3)$$

In this problem we want to verify that the propagator corresponding to (2) equals

$$\Delta(p) = \frac{1}{i(2\pi)^4} \frac{1}{p^2 + m^2 - i\epsilon},$$

by evaluating a Feynman diagram in two different ways. Take an external source J



coupling to ϕ according to $J|\phi|^2 = \frac{1}{2}J(\phi_1^2 + \phi_2^2)$ and write down the diagram from the Lagrangians (1) and (2) with the propagators normalized as above. Compare the results.

2.5. Consider the Lagrangian

$$\mathcal{L} = -\frac{1}{2}(\partial_\mu\phi)^2 - \frac{1}{2}m^2\phi^2 - \lambda\phi^3 - g\phi^4 + c\phi, \quad (1)$$

where the last term generates Feynman diagrams with a single line emanating from the vertex, i.e.,

$$\text{---} \times \quad (2)$$

which is sometimes called a “tadpole” diagram. In this problem we show how to deal with such terms diagrammatically (in tree approximation). Denote

$$\text{---} \bigcirc \quad (3)$$

as the sum over all diagrams in which a single line vanishes, i.e.,

$$\text{---} \bigcirc = \text{---} \times + \text{---} \begin{matrix} \nearrow \times \\ \searrow \times \end{matrix} + \text{---} \begin{matrix} \nearrow \times \\ \searrow \times \\ \downarrow \times \end{matrix} \quad (4)$$

Prove the diagrammatic identity

$$\text{---} \bigcirc \text{---} = \text{---} + \text{---} \begin{array}{l} \bigcirc \\ \bigcirc \end{array} + \text{---} \begin{array}{l} \bigcirc \\ \bigcirc \\ \bigcirc \end{array} \quad (5)$$

by arguing that each diagram contributing to the left-hand side of (5) appears on the right-hand side with the same multiplicity. Denoting the left-hand side of (5) by $v \delta^4(p)$, where p is the momentum, show that (5) is equivalent to

$$v = \frac{c}{m^2} - 3\lambda \frac{v^2}{m^2} - 4g \frac{v^3}{m^2}. \quad (6)$$

Calculate the sum of the irreducible self-energy diagrams $\Sigma(p)$ in tree approximation. The diagrams are given below,

$$\boxed{\Sigma} = \text{---} \bigcirc \text{---} + \text{---} \begin{array}{c} \bigcirc \\ \bigcirc \end{array} \text{---} \quad (7)$$

Sum the Dyson equation and show that the full propagator in tree approximation equals

$$\Delta(p) = \frac{1}{i(2\pi)^4} \frac{1}{p^2 + m^2 + 6\lambda v + 12gv^2}, \quad (8)$$

so that the physical mass equals $\sqrt{m^2 + 6\lambda v + 12gv^2}$. Alternatively, show that (6) follows from making a shift $\phi = \phi' + v$ in (1) with v chosen such that the coefficient of the term linear in ϕ' vanishes. Verify that the new Lagrangian gives rise to the propagator (8).

2.6. The Lagrangian of the linear sigma model is

$$\mathcal{L} = -\frac{1}{2}[(\partial_\mu \phi)^2 + (\partial_\mu \sigma)^2] + \frac{1}{4}\mu^2[\phi^2 + (\sigma + v)^2] - g[\phi^2 + (\sigma + v)^2]^2, \quad (1)$$

with $v = \sqrt{\mu^2/(8g)}$. Show that (1) has no term linear in σ , that the pion mass vanishes, and the sigma mass equals $\mu^2 = 8gv^2$. Furthermore, show that the action is invariant under infinitesimal isospin transformations

$$\delta\sigma = 0, \delta\phi = -\mathbf{\Lambda} \times \phi, \quad (2)$$

and under a second set of infinitesimal transformations

$$\delta\sigma = -\phi \cdot \xi, \quad \delta\phi = (\sigma + v)\xi. \quad (3)$$

Substitute $\sigma = \sigma' - v$ and write (2) and (3) in the form of a matrix multiplying a four-component vector (ϕ, σ') . Let K_i be the matrices belonging to the parameters Λ_i , and L_i be the matrices belonging to the parameters ξ_i . Show that these six matrices span the space of antisymmetric 4×4 matrices. Argue that (2) and (3) are just the infinitesimal transformations corresponding to the group $SO(4)$. Construct the Noether currents corresponding to (2) and (3) and show that they constitute vectors and axial-vectors under parity reversal (c.f. (1.76) and (2.55)). Calculate the amplitude for $\pi + \sigma \rightarrow \pi + \sigma$ in tree approximation and verify that it vanishes in the soft-pion limit.

2.7. The Lagrangian for the nonlinear sigma model is

$$\mathcal{L} = -\frac{1}{2} \frac{(\partial_\mu \phi)^2}{(1 + g\phi^2)^2}, \quad (1)$$

where ϕ is a real three-component pseudoscalar field, c.f. (2.54) and (2.55). Show that (1) is invariant under

$$\delta\phi = -\mathbf{\Lambda} \times \phi + (1 - g\phi^2)\xi + 2g(\xi \cdot \phi)\phi,$$

where $\mathbf{\Lambda}$ and ξ are three-component vectors. Calculate the corresponding currents and show that they are conserved. Distinguish three vector and three axial-vector currents associated with $\mathbf{\Lambda}$ and ξ , respectively. Calculate the four-point amplitude with the external lines on the mass-shell (i.e., $p^2 = 0$). Replace ϕ in (1) by a single-component field and repeat the calculation of the four-point amplitude. Explain your result.

References

General reading material relevant for chapter 2

S.M. Bilenky, Introduction to Feynman Diagrams (Pergamon Press, Oxford, 1974).
 R.P. Feynman, The Theory of Fundamental Processes (Benjamin, New York, 1962).
 J. Schwinger, Particles, Sources and Fields, Vol. I (Addison-Wesley, Reading, MA, 1970).

For a historical background

O. Klein, Z. Phys. 37 (1926) 895.
 W. Gordon, Z. Phys. 40 (1926) 117, 121.
 P.A.M. Dirac, Rapport du 7ième Conseil Solvay de Physique, Structure et Propriétés Noyaux Atomiques (1934) 203.
 H. Yukawa, Proc. Phys. Math. Soc. Japan 17 (1935) 48.

The early papers on meson theory are reprinted in Suppl. Prog. Theor. Phys. 1 (1955) 1.

E. Segré, From X-rays to Quarks (Freeman, San Francisco, 1980).

Many interesting articles can be found in: The Birth of Particle Physics, eds. L.M. Brown and L. Hoddeson (Cambridge University Press, 1983).

For the introduction of the concept of isobaric spin

W. Heisenberg, Z. Phys. 77 (1932) 1.

Some of the necessary mathematics may be found in

P. Dennery and A. Krzywicki, Mathematics for Physicists (Harper and Row, New York, 1967).

S.C. Saxena and S.M. Shah, Introduction to Real Variable Theory (Prentice Hall, New Delhi, (1980),

For sigma models and chiral invariance

M. Gell-Mann and M. Lévy, Nuovo Cim. 16 (1960) 705.

B.W. Lee, Chiral Dynamics (Gordon and Breach, New York, 1972).

S.B. Treiman, R. Jackiw and D.J. Gross, Lectures on Current Algebra and its Applications (Princeton University Press, 1972).

For the Dyson equation

F.J. Dyson, Phys. Rev. 75 (1949) 1736.